Acta Crystallographica Section F
Structural Biology and Crystallization Communications
ISSN 1744-3091

Crystallization and preliminary structural analysis of the *Listeria monocytogenes* Ca^{2+}-ATPase LMCA1

Jacob Lauwring Andersen,[a,b] Pontus Gourdon,[a,b] Jesper Vuust Møller,[a,c] Jens Preben Morth[a]*‡ and Poul Nissen[a,b]*

[a]Centre for Membrane Pumps in Cells and Disease – PUMPKIN, University of Aarhus, Gustav Wieds Vej 10C, 8000 Aarhus C, Denmark, [b]Department of Molecular Biology, University of Aarhus, Gustav Wieds Vej 10C, 8000 Aarhus C, Denmark, and [c]Department of Physiology and Biophysics, University of Aarhus, Ole Worms Allé 6, 8000 Aarhus C, Denmark

‡ Present address: Centre for Molecular Medicine Norway, Nordic EMBL Partnership, University of Oslo, PO Box 1137, Blindern, N-0318 Oslo, Norway.

Correspondence e-mail: j.p.morth@ncmm.uio.no, pn@mb.au.dk

Received 8 April 2011
Accepted 24 April 2011

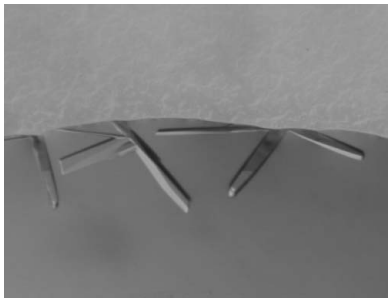

© 2011 International Union of Crystallography
All rights reserved

Ca^{2+}-ATPases are ATP-driven membrane pumps that are responsible for the transport of Ca^{2+} ions across the membrane. The *Listeria monocytogenes* Ca^{2+}-ATPase LMCA1 has been crystallized in the Ca^{2+}-free state stabilized by AlF_4^-, representing an occluded E2–P_i-like state. The crystals belonged to space group $P2_12_12$ and a complete data set extending to 4.3 Å resolution was collected. A molecular-replacement solution was obtained, revealing type I packing of the molecules in the crystal. Unbiased electron-density features were observed for AlF_4^- and for shifts of the helices, which were indicative of a reliable structure determination.

1. Introduction

Ca^{2+}-ATPases are integral membrane proteins that are responsible for the transport of Ca^{2+} ions across the membrane by a mechanism coupled to ATP hydrolysis. They maintain a low intracellular Ca^{2+} concentration (in the micromolar range) which is critical for general Ca^{2+} homeostasis in both prokaryotes and eukaryotes (Campbell, 1983). The Ca^{2+}-ATPases belong to subgroup II of the P-type ATPase family (Axelsen & Palmgren, 1998), which also encompasses the well studied sarcoplasmic reticulum Ca^{2+}-ATPase (SERCA1a; Møller *et al.*, 2010). The Ca^{2+}-ATPases generally contain ten transmembrane helices (M1–10) and three cytoplasmic domains: an actuator domain (A-domain; an N-terminal extension and an insert between M2 and M3) and a phosphorylation domain (P-domain) and nucleotide domain (N-domain) (insert between M4 and M5), with the N-domain protruding from the P-domain. The hallmark of the P-type ATPase family is the formation of a high-energy phosphoenzyme intermediate that targets a conserved aspartic acid side chain in the P-domain during the functional cycle (Charnock & Post, 1963). There is a widespread distribution of open reading frames encoding putative Ca^{2+}-ATPases in the increasing number of sequenced prokaryotic genomes (Faxén *et al.*, 2011). However, their functions *in vivo* remain poorly described. *Listeria monocytogenes* is a Gram-positive facultative intracellular pathogen and a leading cause of death from foodborne bacterial pathogens. Fatal infections, although infrequent, mainly affect immunocompromised people and are associated with high mortality (up to 30% of infected patients; Ramaswamy *et al.*, 2007). The bacterium thrives in very diverse environments ranging from soil to the cytosol of the host cell (Freitag *et al.*, 2009). Alkaline pH is well tolerated and the bacterium continues to grow at pH 9 (Vasseur *et al.*, 2001). The gene locus *lmo0841* of *L. monocytogenes* represents the bacterial class of Ca^{2+}ATPases and is up-regulated in response to alkaline pH (Giotis *et al.*, 2008). The enzyme, named *L. monocytogenes* Ca^{2+}-ATPase 1 (LMCA1), displays Ca^{2+}-dependent ATPase activity and calcium transport with proton counter-transport. The enzyme displays an alkaline pH optimum and this was explained in part by a conserved arginine residue at the intramembraneous ion-binding site possibly acting as a pH sensor (Faxén *et al.*, 2011). The LMCA1 homologue in *Streptococcus pneumoniae*, CaxP, is vital for the survival of this pathogen at the high extracellular Ca^{2+} concentrations in the infected host (Rosch *et al.*, 2008). This emphasizes the importance of understanding the molecular mechanism of the bacterial Ca^{2+}-ATPases and highlights the potential of these transporters as drug targets.

2. Materials and methods

2.1. Protein purification

LMCA1 (locus tag *lmo0841*) was purified as described previously (Faxén *et al.*, 2011). Size-exclusion chromatography (SEC) was performed on a 7.5 mm (internal diameter) × 60 cm TSKgel G3000SW (Tosoh Bioscience) column in SEC buffer: 100 m*M* 3-(*N*-morpholino)-propanesulfonic acid (MOPS) adjusted to pH 6.8 with KOH, 80 m*M* KCl, 20%(*v*/*v*) glycerol, 5 m*M* *β*-mercaptoethanol, 3 m*M* $MgCl_2$ and 0.25 mg ml^{-1} octaethylene glycol monododecyl ether ($C_{12}E_8$; Nikko Chemicals) at 277 K. Fractions containing LMCA1 were concentrated by ultrafiltration to 15 mg ml^{-1} (Vivaspin 20, 50 kDa cutoff), aliquoted and either flash-frozen in liquid N_2 or used immediately.

2.2. LMCA1 re-lipidation and crystallization

Prior to crystallization, LMCA1 (15 mg ml^{-1}) was re-lipidated with 1,2-dioleoyl-*sn*-glycero-3-phosphocholine (DOPC; Avanti Polar Lipids). A weight ratio of 1:3 DOPC:$C_{12}E_8$ was achieved by adding LMCA1 to a glass tube pre-treated with a thin DOPC film. The weight ratio was calculated assuming all-micellar $C_{12}E_8$ being concentrated with LMCA1 in the ultrafiltration step (Jidenko *et al.*, 2005). The lipid film was generated by dispensing DOPC dissolved in $CHCl_3$ into the glass tube and evaporating the $CHCl_3$ in an N_2 atmosphere, thus preventing oxidation. LMCA1 was re-lipidated overnight at 277 K with stirring. Insoluble DOPC and aggregated LMCA1 were removed by centrifugation at 190 000*g* for 10 min. LMCA1 was incubated with 2 m*M* ethylene glycol-bis(2-aminoethyl-ether)-*N*,*N*,*N*′,*N*′-tetraacetic acid (EGTA), 1 m*M* $AlCl_3$ and 10 m*M* NaF to trap it in an occluded E2–AlF_4^- state (Olesen *et al.*, 2007). Initial screening was performed using in-house polyethylene glycol (PEG) screens, in which 1 µl LMCA1 (10 mg ml^{-1} in SEC buffer) was mixed with 1 µl reservoir solution on glass cover slips and equilibrated against 500 µl reservoir solution using the hanging-drop vapour-diffusion method. The setup was sealed with immersion oil (Merck) and equilibrated at 292 K. An initial crystal hit was obtained with 14%(*w*/*v*) PEG 6000, 10%(*v*/*v*) glycerol, 0.1 *M* $MgCl_2$ and 3% *t*-butanol) and was optimized with *n*-decyl-*N*,*N*-dimethyl-3-ammonio-1-propanesulfonate (Z3-10; Sigma) as an additive.

2.3. Data collection and refinement

Crystals were mounted from the mother liquor in nylon loops and were flash-cooled in liquid N_2. A complete data set was collected at 100 K on the X06SA beamline at the Swiss Light Source (SLS) using a PILATUS 6M detector (Dectris). The diffraction images were processed using *XDS* (Kabsch, 2010). Molecular replacement was performed with the program *Phaser* (McCoy *et al.*, 2007) using search models derived from rabbit SERCA1a in proton-occluded E2–P_i representative forms (PDB entries 1wpg, 3fgo, 1xp5, 3b9r and 2zbg; Toyoshima *et al.*, 2004, 2007; Laursen *et al.*, 2009; Olesen *et al.*, 2004, 2007) following rationales described for low-resolution data and low-homology search models (Pedersen *et al.*, 2010). Rigid-body refinement, calculation of OMIT maps and restrained refinement were performed in the *PHENIX* suite (Afonine *et al.*, 2005). Model building and analysis was performed with *Coot* (Emsley & Cowtan, 2004).

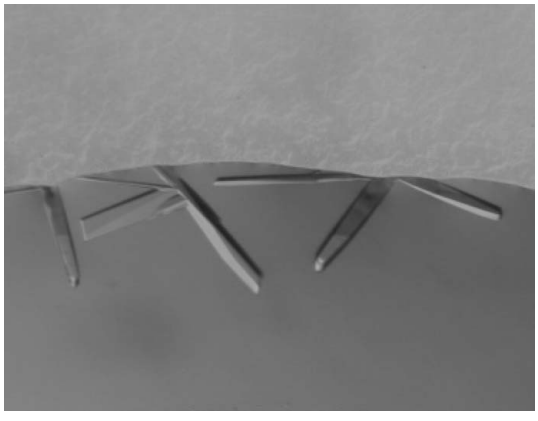

Figure 1
Crystals of the *L. monocytogenes* Ca^{2+}-ATPase LMCA1. Crystals were obtained by the hanging-drop vapour-diffusion method and grew to dimensions of 50 × 50 × 200 µm in two weeks.

3. Results and discussion

3.1. Purification and crystallization of LMCA1

LMCA1 was heterologously expressed in *Escherichia coli* and purified from solubilized membranes by immobilized metal-affinity chromatography as described previously (Faxén *et al.*, 2011). LMCA1 eluted as a monomer in size-exclusion chromatography, similar to $C_{12}E_8$-solubilized SERCA1a from rabbit SR membranes (Andersen *et al.*, 1986). Prior to crystallization, LMCA1 was re-lipidated with 1,2-dioleoyl-*sn*-glycero-3-phosphocholine (DOPC) as previously described for SERCA1a expressed in yeast (Jidenko *et al.*, 2005). Excess lipid that was not solubilized by the detergent was removed by ultracentrifugation and LMCA1 was incubated with the Ca^{2+} chelator EGTA and AlF_4^- to mimic the E2–P_i-occluded form as a transition state in dephosphorylation. Initial crystallization conditions were obtained using an in-house polyethylene glycol (PEG) screen (Sørensen *et al.*, 2006) and were further optimized by including *n*-decyl-*N*,*N*-dimethyl-3-ammonio-1-propanesulfonate (Z3-10) as a second detergent, with the final crystallization buffer consisting of

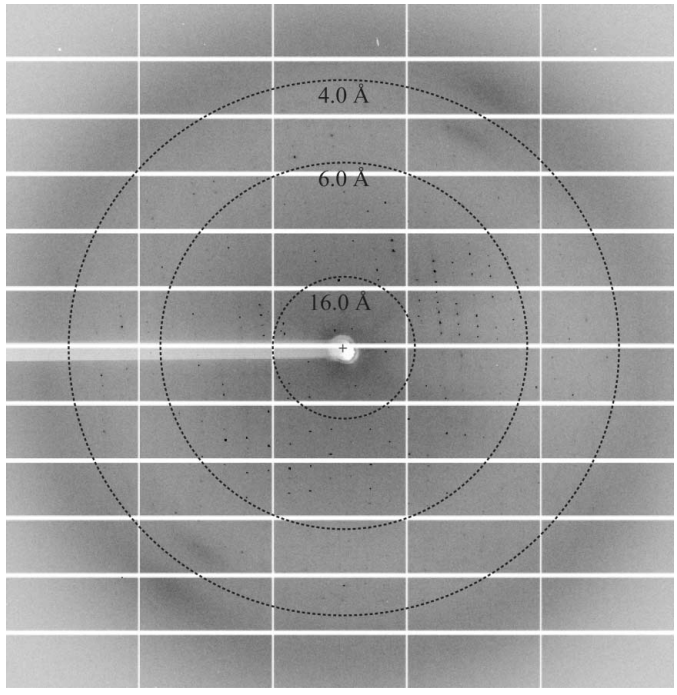

Figure 2
X-ray diffraction pattern of LMCA1 crystals. Resolution circles are indicated by dashed lines.

16%(*w*/*v*) PEG 6000, 14%(*v*/*v*) glycerol, 0.11 *M* $MgCl_2$, 3.75%(*v*/*v*) *t*-butanol, 5 m*M* *β*-mercaptoethanol and 80–160 m*M* (∼2–4 × CMC) *Z*3-10 mixed with the protein sample in 1 + 1 µl drops. Crystals grew to dimensions of 50 × 50 × 200 µm in hanging drops equilibrated over two weeks at 292 K (Fig. 1).

3.2. Data collection and diffraction analysis

A complete data set consisting of 250 oscillation images (Fig. 2) with 0.5° oscillation and 0.5 s exposure per image was collected on the X06SA beamline at the Swiss Light Source (Paul Scherrer Institute) and scaled to a maximum resolution of 4.3 Å. The crystals of LMCA1 belonged to the primitive orthorhombic space group $P2_12_12$, with unit-cell parameters $a = 181.1$, $b = 69.2$, $c = 124.2$ Å. The data statistics are summarized in Table 1.

3.3. Structure determination and analysis

The atomic coordinates of all published SERCA1a structures representing the occluded E2–P_i functional state were tested as search models to obtain initial phases by molecular replacement (MR). The highest translation-function *Z* score (TF *Z* = 10.9) was obtained with SERCA1a stabilized by the inhibitor thapsigargin, ADP and MgF_4^{2-} (PDB entry 1wpg; Toyoshima *et al.*, 2004). The MR solution contained one molecule in the asymmetric unit and showed a type I membrane-protein crystal packing (Michel, 1983) with continuous bilayers of transmembrane domains (Fig. 3). This type I packing is also observed for re-lipidated SERCA1a (Jidenko *et al.*, 2005) and in general for ATPases solubilized from native tissue: SERCA1a (Toyoshima *et al.*, 2000; Sørensen *et al.*, 2004) and Na^+,K^+-ATPase (Morth *et al.*, 2007). The molecular-replacement solution was subjected to rigid-body and limited restrained refinement ($R = 44.1\%$ and $R_{free} = 47.4\%$). Unbiased $F_o - F_c$ electron density (30–4.3 Å resolution, 5σ peak level) was observed at the position of the excluded MgF_4^{2-} ligand of the search model, suggesting the presence of AlF_4^- bound to LMCA1 (Fig. 4) and validating the solution. Furthermore, unbiased electron-density maps suggested minor rearrangements in the position of secondary-structure elements such as the M2 helix (Fig. 5). Poor electron density was observed for the N-domain, which appears to be rather disordered in the structure.

Table 1
Data-collection and processing statistics.

Values in parentheses are for the highest resolution shell.

Beamline	X06SA, SLS
Wavelength (Å)	0.9998
Detector	PILATUS 6M
Crystal-to-detector distance (mm)	670.0
Rotation range per image (°)	0.5
Total rotation range (°)	125
Resolution range (Å)	30–4.3 (4.4–4.3)
Space group	$P2_12_12$
Unit-cell parameters (Å)	$a = 181.1$, $b = 69.2$, $c = 124.2$
Mosaicity (°)	0.14
Total No. of measured reflections	97149
Unique reflections	11128
Multiplicity	8.7
Mean $I/\sigma(I)$	9.8 (2.7)
Completeness (%)	99.9 (99.6)
R_{meas}† (%)	15.4 (96.5)
$R_{merge\text{-}F}$† (%)	15.9 (57.7)
Molecules per asymmetric unit‡	1
Matthews coefficient‡ (Å^3 Da^{-1})	4.1
Solvent content‡ (%)	70.0

† The quality of the individual intensity observations and the reduced structure-factor amplitudes are evaluated by R_{meas} and $R_{merge\text{-}F}$, respectively. $R_{meas} = \sum_h [n_h/(n_h-1)]^{1/2} \sum_i^{n_h} |\langle I_h\rangle - I_{h,i}| / \sum_h \sum_i^{n_h} I_{h,i}$, where n_h is the multiplicity, $I_{h,i}$ is the *i*th intensity of reflection *h* and $\langle I_h\rangle$ is the weighted average intensity for all observations *i* of reflection *h*. $R_{merge\text{-}F} = (\sum |A_{I_{h,P}} - A_{I_{h,Q}}|)/(\frac{1}{2}\sum A_{I_{h,P}} - A_{I_{h,Q}})$, where $I_{h,P}$ and $I_{h,Q}$ represent the partially averaged intensities (Diederichs & Karplus, 1997). ‡ The most probable solution according to statistical sampling (Kantardjieff & Rupp, 2003).

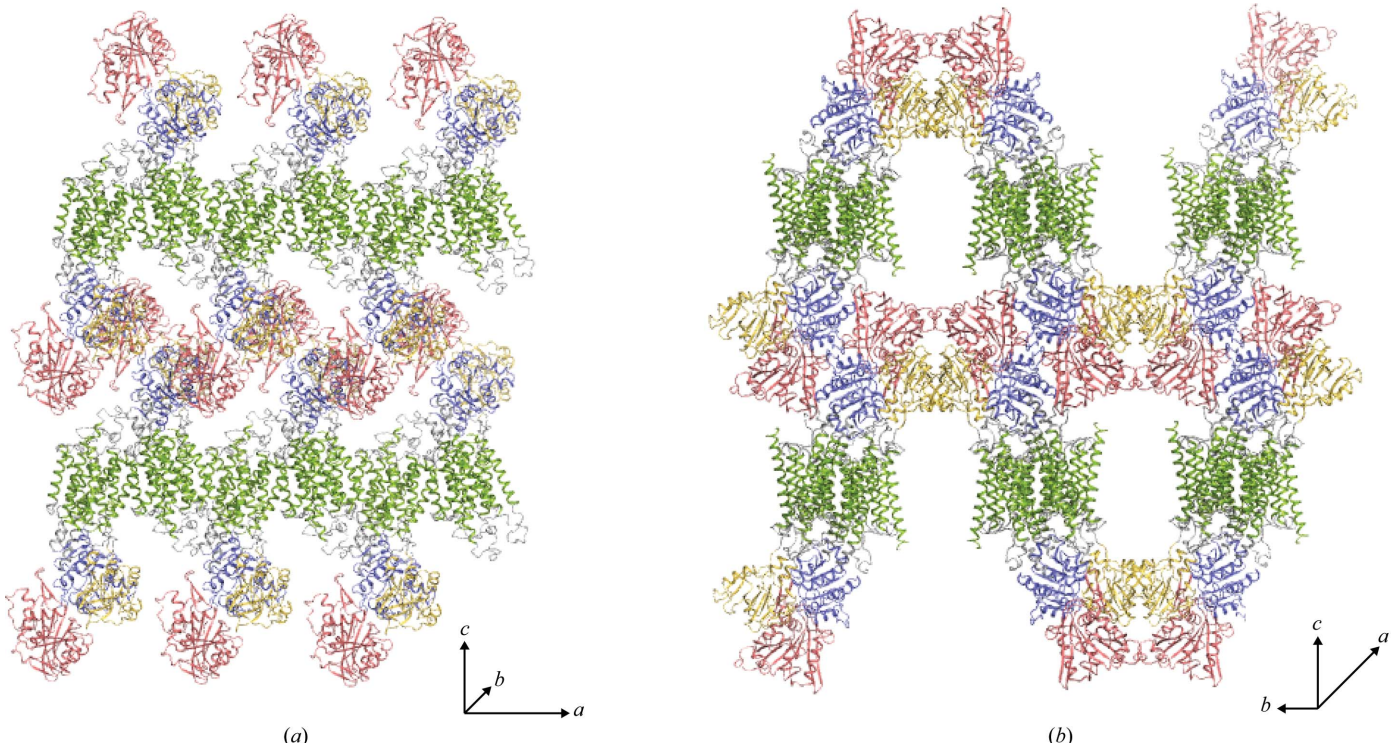

Figure 3
Packing of LMCA1 in the primitive orthorhombic space group $P2_12_12$. (*a*) The transmembrane helices are depicted in green and the A-domain, P-domain and N-domain are shown in yellow, blue and red, respectively. (*b*) View rotated 90° along the *c* axis. This figure and Figs. 4 and 5 were prepared using *PyMOL* (v.1.3; Schrödinger LLC; http://www.pymol.org).

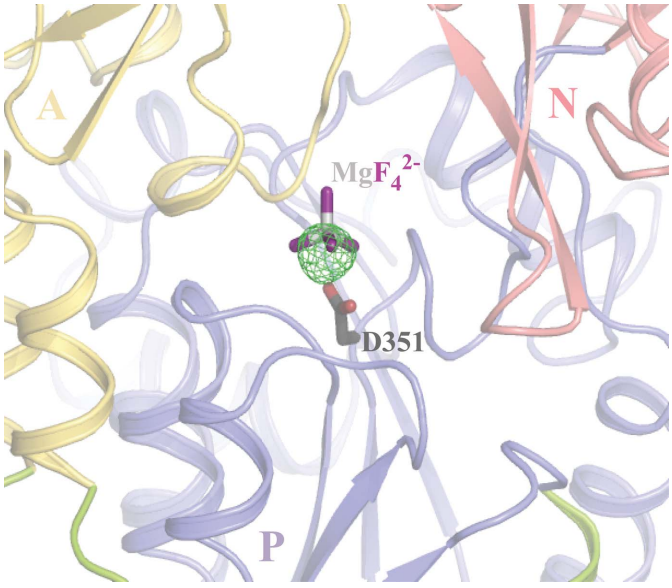

Figure 4
LMCA1 was crystallized in the E2–P_i-like state with AlF_4^- as a transition-state mimic of dephosphorylation. Following rigid-body and restrained refinement, a strong peak appeared at the position of the excluded MgF_4^{2-} ligand of the search model in the $F_o - F_c$ difference Fourier map as depicted by a 5.0σ contour level shown as a green mesh. The canonical aspartic acid phosphorylation site is shown in stick representation, with MgF_4^{2-} in light grey (Mg) and purple (F). The secondary-structure elements are coloured as in Fig. 3.

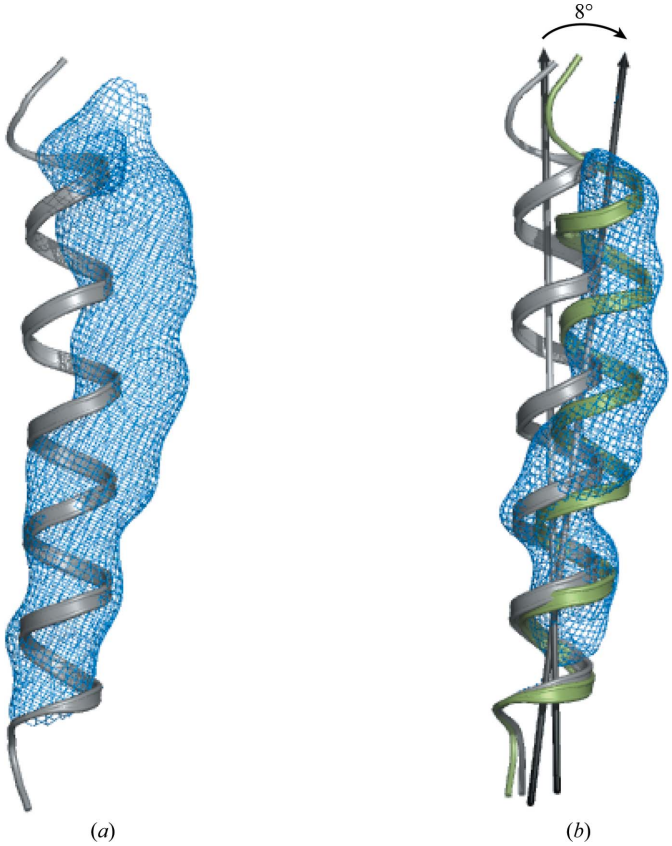

Figure 5
(*a*) $2F_o - F_c$ electron-density map of the transmembrane helix 2 region contoured at 1.5σ (blue) following the initial rigid-body refinement. (*b*) OMIT electron-density map contoured at 2.0σ (blue) calculated with M2 excluded during refinement and map calculation. The position of M2 following the initial rigid-body refinement (*a*) is depicted in grey and the position following model rebuilding and restrained refinement is depicted in green.

However, it also has the lowest sequence identity of the domains compared with the SERCA1a search model (28% compared with 38% overall), with truncations and deletions of secondary-structure elements and loop regions, which may in part explain this observation. From our preliminary structural analysis we conclude that the E2–AlF_4^- form of LMCA1 adopts an occluded structure, as observed for SERCA1a. However, higher resolution studies will be required to reveal important details of the conserved arginine residue in the membrane, possibly relating to a pH-sensing role, which is characteristic of a large group of bacterial Ca^{2+}-ATPases (Faxén *et al.*, 2011). Crystal optimization to achieve higher resolution is now in progress, including mutational studies to further stabilize LMCA1 in the E2–P_i state and selenomethionine incorporation to obtain experimental phases.

We are grateful to Anna Marie Nielsen, Karen Marx and Birte Nielsen for technical assistance, and to Anne-Marie Lund Winther, Bertrand Arnou and Claus Olesen for advice and stimulating discussions. We would like to thank the Swiss Light Source (Paul Scherrer Institute), European Synchrotron Facility and MAX-lab for providing data-collection facilities and for excellent support. The work was supported by a Center of Excellence grant from the Danish National Research Foundation. PG was supported by a postdoctoral fellowship from The Swedish Research Council, JPM was supported by Lundbeckfonden and Carlsbergfondet, and PN was supported by a Hallas–Møller stipend of the Novo Nordisk Foundation.

References

Afonine, P. V., Grosse-Kunstleve, R. W. & Adams, P. D. (2005). *CCP4 Newsl.* **42**, contribution 8.
Andersen, J. P., Vilsen, B., Nielsen, H. & Møller, J. V. (1986). *Biochemistry*, **25**, 6439–6447.
Axelsen, K. B. & Palmgren, M. G. (1998). *J. Mol. Evol.* **46**, 84–101.
Campbell, A. K. (1983). *Intracellular Calcium: Its Universal Role as Regulator*. New York: John Wiley & Sons.
Charnock, J. S. & Post, R. L. (1963). *Nature (London)*, **199**, 910–911.
Diederichs, K. & Karplus, P. A. (1997). *Nature Struct. Mol. Biol.* **4**, 269–275.
Emsley, P. & Cowtan, K. (2004). *Acta Cryst.* D**60**, 2126–2132.
Faxén, K., Andersen, J. L., Gourdon, P., Fedosova, N., Morth, J. P., Nissen, P. & Møller, J. V. (2011). *J. Biol. Chem.* **286**, 1609–1617.
Freitag, N. E., Port, G. C. & Miner, M. D. (2009). *Nature Rev. Microbiol.* **7**, 623–628.
Giotis, E. S., Muthaiyan, A., Blair, I. S., Wilkinson, B. J. & McDowell, D. A. (2008). *BMC Microbiol.* **8**, 102.
Jidenko, M., Nielsen, R. C., Sørensen, T. L., Møller, J. V., le Maire, M., Nissen, P. & Jaxel, C. (2005). *Proc. Natl Acad. Sci. USA*, **102**, 11687–11691.
Kabsch, W. (2010). *Acta Cryst.* D**66**, 125–132.
Kantardjieff, K. A. & Rupp, B. (2003). *Protein Sci.* **12**, 1865–1871.
Laursen, M., Bublitz, M., Moncoq, K., Olesen, C., Møller, J. V., Young, H. S., Nissen, P. & Morth, J. P. (2009). *J. Biol. Chem.* **284**, 13513–13518.
McCoy, A. J., Grosse-Kunstleve, R. W., Adams, P. D., Winn, M. D., Storoni, L. C. & Read, R. J. (2007). *J. Appl. Cryst.* **40**, 658–674.
Michel, H. (1983). *Trends Biochem. Sci.* **8**, 56–59.
Møller, J. V., Olesen, C., Winther, A. M. & Nissen, P. (2010). *Q. Rev. Biophys.* **43**, 501–566.
Morth, J. P., Pedersen, B. P., Toustrup-Jensen, M. S., Sørensen, T. L., Petersen, J., Andersen, J. P., Vilsen, B. & Nissen, P. (2007). *Nature (London)*, **450**, 1043–1049.
Olesen, C., Picard, M., Winther, A. M., Gyrup, C., Morth, J. P., Oxvig, C., Møller, J. V. & Nissen, P. (2007). *Nature (London)*, **450**, 1036–1042.
Olesen, C., Sørensen, T. L., Nielsen, R. C., Møller, J. V. & Nissen, P. (2004). *Science*, **306**, 2251–2255.
Pedersen, B. P., Morth, J. P. & Nissen, P. (2010). *Acta Cryst.* D**66**, 309–313.
Ramaswamy, V., Cresence, V. M., Rejitha, J. S., Lekshmi, M. U., Dharsana, K. S., Prasad, S. P. & Vijila, H. M. (2007). *J. Microbiol. Immunol. Infect.* **40**, 4–13.
Rosch, J. W., Sublett, J., Gao, G., Wang, Y.-D. & Tuomanen, E. I. (2008). *Mol. Microbiol.* **70**, 435–444.

Sørensen, T. L., Møller, J. V. & Nissen, P. (2004). *Science*, **304**, 1672–1675.
Sørensen, T. L., Olesen, C., Jensen, A. M., Møller, J. V. & Nissen, P. (2006). *J. Biotechnol.* **124**, 704–716.
Toyoshima, C., Nakasako, M., Nomura, H. & Ogawa, H. (2000). *Nature (London)*, **405**, 647–655.
Toyoshima, C., Nomura, H. & Tsuda, T. (2004). *Nature (London)*, **432**, 361–368.
Toyoshima, C., Norimatsu, Y., Iwasawa, S., Tsuda, T. & Ogawa, H. (2007). *Proc. Natl Acad. Sci. USA*, **104**, 19831–19836.
Vasseur, C., Rigaud, N., Hébraud, M. & Labadie, J. (2001). *J. Food Prot.* **64**, 1442–1445.